51st AIAA/ASME/ASCE/AHS/ASC Structures, Structural Dynamics, and Materials Conference
 18th
12 - 15 April 2010, Orlando, Florida

AIAA 2010-2558

2010 AIAA SDM Student Symposium

Mistuning Identification of Blisks at Higher Frequencies

Andrew C. Madden,* Matthew P. Castanier,† and Bogdan I. Epureanu‡

University of Michigan, Ann Arbor, Michigan 48109-2125

There is a large body of research on reduced-order modeling of bladed disks and integrally bladed disks (blisks) for predicting the mistuned vibration response. However, most work to date has focused on the lower frequency families of blade-dominated modes. Relatively few studies have considered the response in higher frequency regions that feature more complex blade motions and more closely spaced families of modes. Moreover, some reduced-order modeling techniques for mistuned blisks make use of simplifications inherent in lower frequency ranges and neglect complexities of higher frequency ranges. In this study, key challenges of higher frequency regimes are considered. Procedures are presented and evaluated for reduced-order modeling and mistuning identification of blisks at frequency ranges beyond the first few families of blade-dominated modes. It is shown that mistuning patterns can be identified for higher mode families, and the mistuning pattern for each family is generally unique when the physical mistuning is not uniform throughout each blade. Finally, a procedure to choose appropriate measurement points for modeling and mistuning identification is proposed.

I. Introduction

STRUCTURES that consist of a cyclic assembly of identical substructures are said to possess cyclic symmetry. The design of a single stage of a turbomachinery rotor, or bladed disk, typically features cyclic symmetry. Using cyclic symmetry routines in commercial finite element software enables one to analyze the entire bladed disk using a model of only one sector, which results in considerable reduction of computational costs.

However, there are always small structural deviations among blades, called mistuning. Although mistuning is typically small (e.g., blade-alone natural frequency variations of 1–5%), it can lead to a dramatic increase in maximum blade stress and is a major driver for high cycle fatigue in turbine engines. From a modeling perspective, mistuning destroys the cyclic symmetry, such that the full bladed disk needs to be modeled. Therefore, several efficient approaches for reduced-order modeling of mistuned bladed disks have been developed.[1–7]

These reduced-order models treat mistuning as a variation in natural frequencies for one or more modes of an isolated blade. For bladed disks with inserted blades, one can measure the natural frequencies of manufactured blades directly. However, this is not possible with integrally bladed disks (blisks), which are becoming more prevalent in newer and next-generation engines. For blisks, several mistuning identification methods have been developed that use experimental response data for the full blisk in order to extract individual blade mistuning parameters. These methods range from techniques based on lumped parameter models[8,9] to more advanced approaches requiring information from a finite element model.[10–22]

The combination of work on modeling and identification of mistuning in blisks has made it possible to accurately model blisks at a fraction of the computational cost compared to finite element analysis. However, in general, the current techniques have only been validated for predictions in lower frequency ranges.

In higher frequency ranges, one is more likely to observe system modes that feature a combination of blade and disk motion. Moreover, it is more likely that the blade portion of system normal modes will respond like a combination of blade-alone mode shapes rather than one single mode shape. Another difficulty with higher frequencies is the localization of motion in certain portions of the blade. At lower frequencies, the motion of the response is relatively uniform throughout the blade. Also, it is generally assumed that mistuning is constant for the entire blade. However,

*Graduate Student Research Assistant, Department of Mechanical Engineering. Student Member of AIAA.
†Adjunct Associate Research Scientist, Department of Mechanical Engineering. Senior Member of AIAA.
‡Associate Professor, Department of Mechanical Engineering.

the physical sources of mistuning (e.g., variation in blade thickness from the nominal design) are generally not uniform throughout the blade, and therefore the mistuning pattern changes for different blade-alone mode shapes if they feature motion in different regions of the blade. This is important for higher frequency modes as blades exhibit motion localized to smaller regions.

Most reduced-order modeling methods to date have not addressed the issues specific to mistuning in higher frequency ranges. In fact, some methods are specifically formulated for isolated, lower-frequency families of blade-dominated modes.[17] One exception is the component mode mistuning (CMM) method developed by Lim et al.,[6,7] which allows different mistuning patterns for different blade-alone modes. The method was validated numerically for a higher frequency range with two overlapping families of blade-dominated modes.[7] However, the CMM-based mistuning identification method[19–21] has only been validated in lower frequency ranges.

This work is an extension of previous work by the authors[23] on improving robustness of the CMM-based mistuning identification technique. The previous work considered only lower frequency regimes. The focus of this work is to extend CMM-based mistuning identification to higher frequency ranges. First, this work will consider the identification of multiple mistuning patterns. Demonstrating that the mistuning identification method can identify multiple mistuning patterns ensures that the appropriate mistuning parameters can be identified for the realistic case of non-uniform physical mistuning in each blade. Next, this work tackles the issue of selecting measurement points to use for mistuning identification which considers the vibration of smaller regions of the blade for higher modes. To this end, the effective independence distribution vector (EIDV)[24,25] method is used in an iterative approach to identify measurement points that yield the highest accuracy for mistuning identification given a limited amount of measurement data to be collected.

II. Theory

A. Multiple Mistuning Patterns

The governing equation for a mistuned blisk in tuned system modal coordinates has been expressed by Lim et al.[7] for the CMM reduced order model neglecting mass mistuning as

$$-\omega^2\mathbf{p} + (1+j\gamma)\left[\mathbf{\Lambda}^s + \mathbf{\Lambda}^{\delta,s} + \mathbf{\Phi}^{s^{\mathrm{T}}}\mathbf{K}^\delta\mathbf{\Phi}^s\right]\mathbf{p} = \mathbf{f}^s, \tag{1}$$

where ω is the response frequency of the system, $\mathbf{p}$ represents the system modal coordinates, $\mathbf{\Lambda}^s$ are the tuned system eigenvalues, $\mathbf{\Phi}^s$ is the blade portion of the tuned system mode shapes, and $\mathbf{f^s}$ is the modal forcing vector. The diagonal matrix $\mathbf{\Lambda}^{\delta,s}$ contains the differences in the eigenvalues of the assumed nominal tuned system and the actual tuned system as suggested in Lim et al.[19,20], and referred to as cyclic modeling error. This equation can be simplified by assuming that the blade portion of the tuned mode shapes can be represented as a linear combination of cantilevered blade mode shapes as follows

$$\begin{aligned} -\omega^2\mathbf{p} + (1+j\gamma)\left[\mathbf{\Lambda}^s + \mathbf{\Lambda}^{\delta,s} + \mathbf{q}^{\mathrm{T}}\Phi^{cb^{\mathrm{T}}}\mathbf{K}^\delta\mathbf{\Phi}^{cb}q\right]\mathbf{p} &= \mathbf{f}^s, \\ -\omega^2\mathbf{p} + (1+j\gamma)\left[\mathbf{\Lambda}^s + \mathbf{\Lambda}^{\delta,s} + \mathbf{q}^{\mathrm{T}}\mathbf{\Lambda}^{\delta,cb}\mathbf{q}\right]\mathbf{p} &= \mathbf{f}^s, \end{aligned} \tag{2}$$

where $\mathbf{q}$ represents the participation the cantilevered blade mode shape in the system blade mode shape, and $\mathbf{\Phi}^{cb}$ are the cantilevered blade modes shapes. The change in the cantilevered blade eigenvalues between the tuned and mistuned blisks is $\mathbf{\Lambda}^{\delta,cb}$.

The use of cantilevered blade mode shapes to represent the blade portion of system modes implies that mistuning appears in the equations as $\mathbf{\Lambda}^{\delta,cb}$. This also means that one tuned system normal mode (blade portion) can be represented as a linear combination of multiple cantilevered blade mode shapes. At lower frequencies, modes tend to be closely spaced in frequency, and the blade motion can be well represented by the cantilevered blade mode shape. As frequencies increase and veerings become more common, the motion of the blades can be a complicated combination of multiple cantilevered blade mode shapes. Therefore, to obtain accurate predictions, one should include as many cantilevered blade mode shapes as necessary to predict the blade portion of the system normal mode. The diagonal matrix $\mathbf{\Lambda}^{\delta,cb}$ contains the deviations of the cantilevered blade eigenvalues from their nominal. In the case where multiple cantilevered blade normal modes are needed to represent the blade portion of the system normal mode, the matrix has multiple entries for each blade. This corresponds to eigenvalue deviations for each blade for each cantilevered blade mode used. This formulation accounts for the cases where mistuning is manifested differently for each cantilevered blade mode shape, and leads to an accurate reduced-order model.

Additionally, one may relate mistuning to localized regions in the geometry. Consider the geometry of a blade divided into N regions of interest. Let us assume that a small change in the blade properties at location n is denoted by α_n. The mistuning for mode m for the entire blade caused by local mistuning associated with the n^{th} location in the blade is defined as

$$\Delta\lambda_n{}^m = f^m(\alpha_n) = f^m\mid_{\alpha_n=0} + \left.\frac{df^m}{d\alpha_n}\right|_{\alpha_n=0} \alpha_n + O(\alpha_n{}^2), \tag{3}$$

where f is a complicated, unknown function which is zero for a tuned system. Hence, assuming that mistuning is proportional to the change in the blade, and neglecting higher order terms, Eq. 3 becomes

$$\Delta\lambda_n{}^m = f^m(\alpha_n) = \left.\frac{\partial f^m}{\partial\alpha_n}\right|_{\alpha_n=0} \alpha_n. \tag{4}$$

Similarly, the mistuning for mode m for the entire blade with N mistuning locations can be written using the same assumptions as

$$\Delta\lambda^m = f^m(\boldsymbol{\alpha}) = \left.\frac{\partial f^m}{\partial\alpha_1}\right|_{\boldsymbol{\alpha}=\mathbf{0}} \alpha_1 + \cdots + \left.\frac{\partial f^m}{\partial\alpha_n}\right|_{\boldsymbol{\alpha}=\mathbf{0}} \alpha_N, \tag{5}$$

where $\boldsymbol{\alpha} = [\alpha_1, \ldots, \alpha_N]^T$. If one uses the mistuning identification procedure,[21,23] in general it is possible to determine multiple distinct mistuning patterns related to different blades. Then consider the case when N distinct mistuning values are determined for N modes

$$\begin{aligned} \Delta\lambda^1 &= \left.\frac{\partial f^1}{\partial\alpha_1}\right|_{\boldsymbol{\alpha}=\mathbf{0}} \alpha_1 + \cdots + \left.\frac{\partial f^1}{\partial\alpha_N}\right|_{\boldsymbol{\alpha}=\mathbf{0}} \alpha_N, \\ &\vdots \\ \Delta\lambda^N &= \left.\frac{\partial f^N}{\partial\alpha_1}\right|_{\boldsymbol{\alpha}=\mathbf{0}} \alpha_1 + \cdots + \left.\frac{\partial f^N}{\partial\alpha_N}\right|_{\boldsymbol{\alpha}=\mathbf{0}} \alpha_N, \end{aligned} \tag{6}$$

which yields N equations with N unknowns $\Delta\boldsymbol{\lambda} = \mathbf{C}\cdot\boldsymbol{\alpha}$. At this point, a single blade may be mapped by solving Eq. 4 for the coefficients $C_{ij} = \left.\frac{\partial f^m}{\partial\alpha_n}\right|_{\alpha_n=0}$ denoting the n^{th} location. This mapping may be computed by arbitrarily assuming a local mistuning value and using the mistuning identification procedure to determine the blade mistuning values. This can be done for coefficients 1 through N, which can then be substituted into Eq. 6. Next, the mistuning values of the actual blade with N local mistuning locations can be identified using the CMM procedure. Finally, Eq. 6 can be solved for the local mistuning values $\boldsymbol{\alpha}$.

B. Iterative Measurement Point Selection for Mistuning Identification

The CMM reduced-order model transforms the governing equations from physical coordinates $\mathbf{x}$ to modal coordinates $\mathbf{p}$ in order to reduce the model size using the equation

$$\mathbf{x} = \boldsymbol{\Phi}^s\mathbf{p}, \tag{7}$$

where $\boldsymbol{\Phi}^s$ is the tuned modal matrix (mass normalized). To reduce the size of the model, $\boldsymbol{\Phi}^s$ is truncated to include a select group of modes in the frequency range of interest. For mistuning identification, the physical degrees of freedom (DOF) are measured experimentally. The tuned system normal mode shapes can be found from the finite element model (FEM) of the tuned system. Using this information, the modal coordinates $\mathbf{p}$ can be found.

There are two key reasons why determining the appropriate modal coordinates is difficult. First, only a significantly reduced subset of DOF can be measured because the physical coordinates $\mathbf{x}$ are determined experimentally. This means that DOF must be strategically chosen to best represent the physical motion and thereby the mode shapes. Second, Eq. 7 is a least squares problem when solving for modal coordinates because the number of modes used for the reduced-order model is smaller than the total number of DOF.[23] The quality of the solution of the least squares problem depends on the quality of the measurement points used (in the physical domain).

Since the selection of the reduced DOF to represent the response in the physical domain is important, an algorithm is developed to chose the most appropriate points. Generalizing the work of the authors,[23] the direct reduced-order model (DROM) concept is extended. The previous application of DROMs made use of numerically generated test data

in modal coordinates, in essence creating a set of surrogate data to be used for $\mathbf{p}$. With this information, the system could be interrogated to determine the correct number of tuned system mode shapes $\mathbf{\Phi}^s$ to be used in the model. For the algorithm herein, the current technique is modified to generate surrogate physical data $\mathbf{x}$ to account for the error created in the least squares transformation from physical to modal coordinates. This approach better describes how actual data affects the transformation. In the previous work, the measurement points were chosen using the effective independent distribution vector (EIDV).[24,25] That approach is employed here in an iterative fashion.

The DROM interrogates the system and determines which set of tuned system modes provides the best basis for identifying mistuning. In the previous work, a candidate set of modes were used to determine the EIDV measurement points. However, for each degenerate case of the candidate set of modes, the EIDV measurement points might be less suitable. In this work, the EIDV algorithm is used for each set of possible IROM modes to determine measurement points which are best suited for the identification procedure. Using DROM generated data for all possible EIDV measurement point combinations, each IROM can be interrogated with the optimal set of EIDV measurment points. This provides the best set of measurement points for the best set of basis modes to be used in the mistuning identification procedure.

III. Results

The results presented are related to the tuned finite element model shown in Fig. 1a. The model has two moduli of elasticity shown by different colors. At this point, even though there are multiple material parameters in the model, it is still cyclically symmetric, and therefore tuned. In Fig. 1b, the frequency versus nodal diameter map is shown up to 20 kHz, which is the effective range for the first six cantilevered blade mode families. It is noted that at the higher frequency ranges, significant veering regions are present. These regions make mistuning identification more difficult because of an assumption in the basic CMM formulation that mistuned modes closely spaced in frequency can be represented by tuned modes in that same frequency range, a concept introduced by Yang and Griffin.[26] As veering regions become more dominant, this assumption is violated even in regions of high modal density. Therefore, this system is suitable to test the novel methods proposed herein.

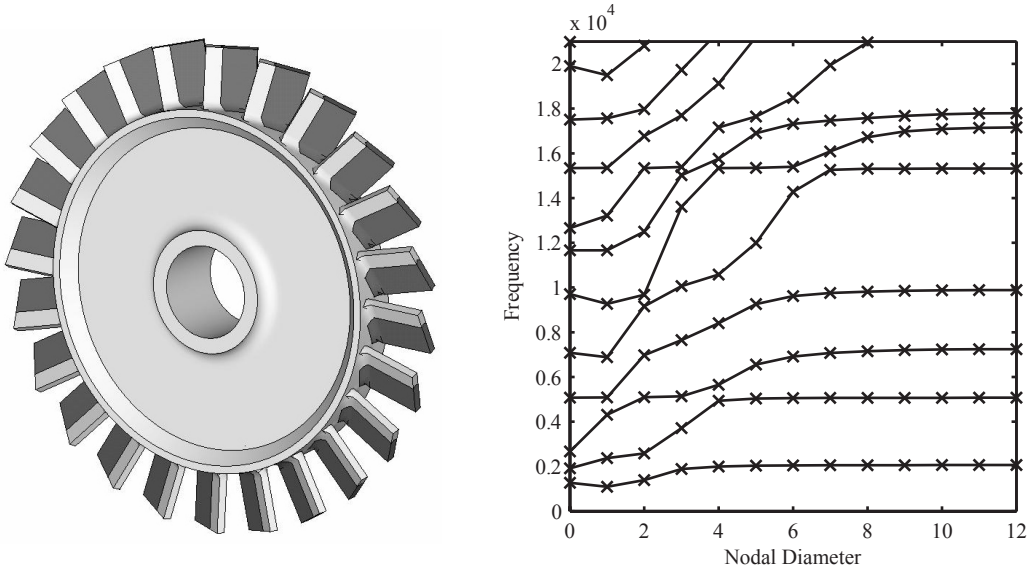

(a) FEM of the blisk with 24 blades.

(b) Frequency vs. Nodal Diameter.

Figure 1. Overview of the tuned FEM of a blisk with 24 blades.

A. Multiple Mistuning Patterns

To demonstrate the approach, multiple mistuning patterns are investigated for the 24-bladed disk in Fig. 1a, which is modified such that the blade portion is divided into four segments with differing modulus of elasity. The subsequent mistuned model generated from the tuned 24-blade disk is shown in Fig 2. Note that each section of the blade has a

distinct random change in modulus of elasticity of under 5%. These physical changes result in a different mistuning pattern for the six different cantilevered blade modes used in the model. This is demonstrated by comparing results for the first cantilevered blade mode family and the fifth in Fig. 3.

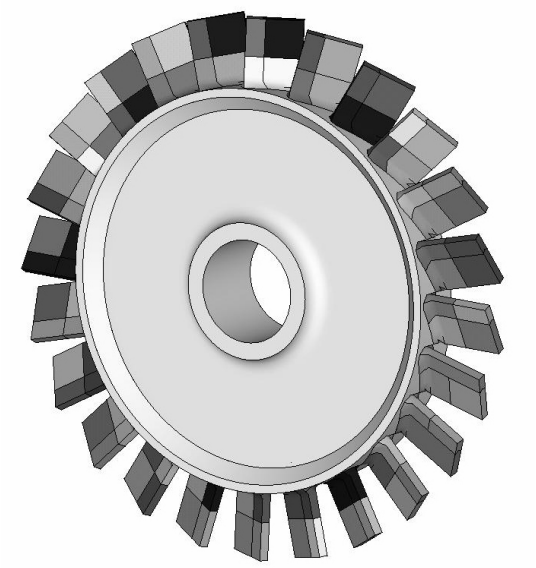

Figure 2. FEM of blisk with multiple mistuning patterns.

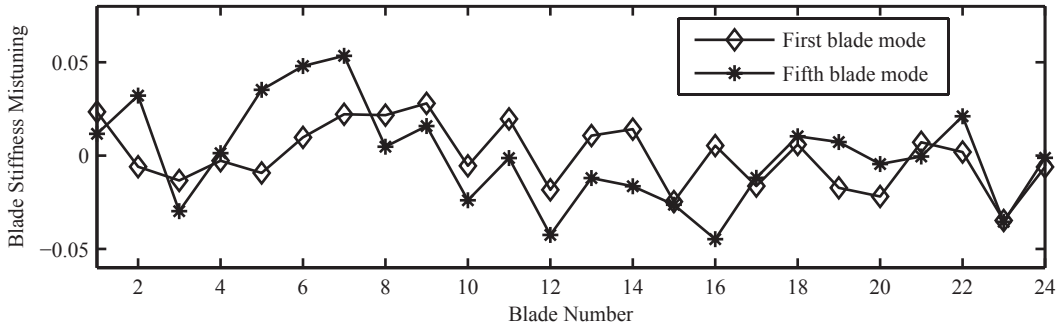

Figure 3. Model updating parameters for 1st and 5th cantilevered blade modes.

To demonstrate the current capabilities of the mistuning identification algorithm, Figs. 4a-4f show that these different mistuning patterns can indeed be identified. It should be noted that the current mistuning identification procedure makes use of a combination of the author's previous work,[23] and the measurement point iteration algorithm which is presented in the following section. It is clear from Figs. 4a-4f that the mistuning can be well identified for each cantilevered blade mode family. Since the last cantilevered blade mode family has a contributions up to 20kHz, the results are sufficient to suggest that mistuning can be identified in higher frequency ranges without significant loss of accuracy. As it is well known that forced response amplitudes of mistuned systems are highly sensitive to mistuning, the ability to identify mistuning and subsequently model mistuning is critical to get accurate predictions. Furthermore, these results demonstrate that six distinct mistuning patterns can be identified, which allows for the modeling of non-proportional mistuning.

Because distinct mistuning patterns exist in this case, it is possible that one may be able to extract information about the location and amount of mistuning from a physical perspective. Consider Fig. 5a and 5b which show the first and six cantilevered blade modes. It is evident that changing the frequencies of each of these cantilevered blade modes will have different effects on the same physical location of the blade. This general idea was employed to back out variations in the modulus of elasticity of four locations on a blade using the mistuning identification. As mentioned in Sec. IIA, it is theoretically possible to identify these four locations with the first four mistuning patterns. However, in practice, this results in the inversion of an ill-conditioned matrix $\mathbf{C}$, which heavily places reliance on the

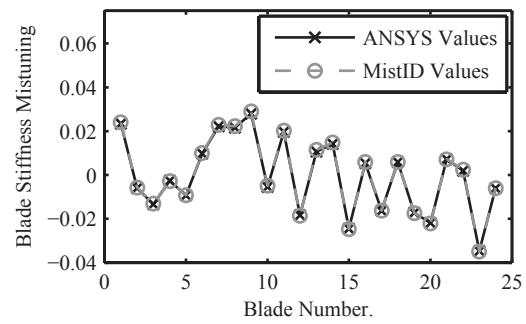

(a) Blade stiffness mistuning for 1st CB mode.

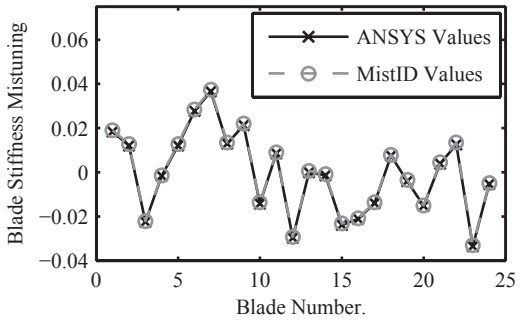

(b) Blade stiffness mistuning for 2nd CB mode.

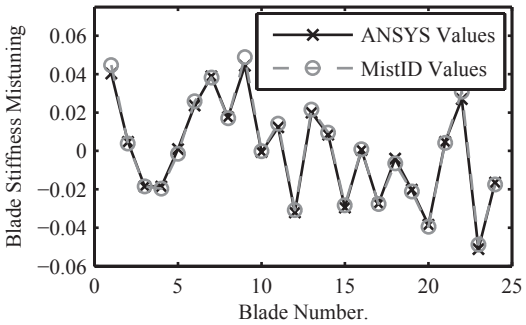

(c) Blade stiffness mistuning for 3rd CB mode.

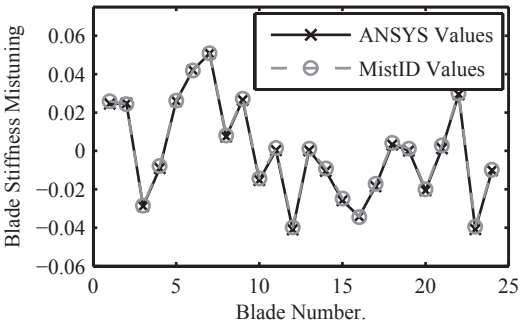

(d) Blade stiffness mistuning for 4th CB mode.

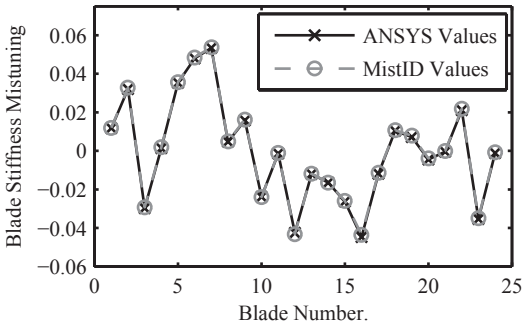

(e) Blade stiffness mistuning for 5th CB mode.

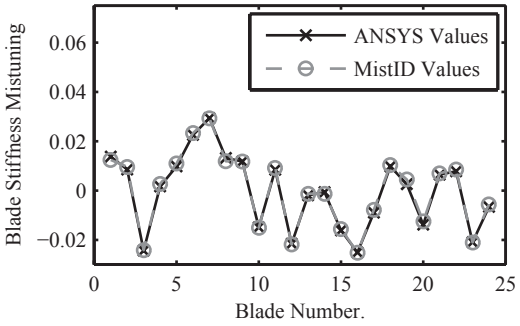

(f) Blade stiffness mistuning for 6th CB mode.

Figure 4. Model updating parameters for 1st through 6th cantilevered blade modes (0-18000 Hz). MistID values represent mistuning values obtained using the proposed mistuning identification approach.

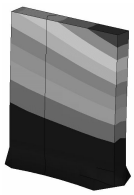

(a) 1st cantilevered blade mode (2106 Hz).

(b) 6th cantilevered blade mode (17861 Hz).

Figure 5. Comparison of the response of blade portions for different CB modes.

accuracy of the mistuning results. Physically, ill conditioning is caused by the fact that the first four cantilevered blade mode families are not distinguishable enough to accurately determine these parameters. As more cantilevered blade mode families are added, additional sensitivity to specific locations of a blade is added. Therefore, to improve the conditioning of matrix $\mathbf{C}$, additional mistuning patterns were identified.

It was determined that only four mistuning patterns are needed to obtain accurate predictions of the physical mistuning. The patterns that were used came from the 1st, 3rd, 5th, and 6th cantilevered blade mode families. The results are shown in Fig. 6. Modulus of elasticity variations were identified for four different locations for each blade. Although the theoretical limit to the number of locations to identify is the number of elements, clearly there are practical limits to the resolution that can be obtained.

In general, a particular set of mistuning patterns is best for identifying the modulus of elasticity variations in the blade. Next, a novel way is proposed to practically determine which mistuning families are needed to obtain accurate predictions. The variations in modulus of elasticity are computed by inverting the coefficient matrix $\mathbf{C}$ as described in Sec. IIA, and multiplying it by mistuning values from various cantilevered blade mode families for a given physical blade. It is rather inexpensive to get the coefficient matrix $\mathbf{C}$ and surrogate mistuning patterns by applying a mistuning pattern to a cantilevered blade and computing the modal frequency. This can done before collecting expensive measurement data. With a greater number surrogate mistuning patterns than the physical locations to be identified and with the corresponding coefficient matrix $\mathbf{C}$, it is possible to compute variations in the modulus of elasticity. By slightly perturbing the mistuning patterns for less than the maximum expected patterns, identifying variations in the modulus of elasticity, and then recomputing the mistuning patterns, one can compute a residual. If the residual is low for all mistuning families, it is likely that the computed variation in modulus of elasticity is correct. However, if the residual is high for any one of the mistuning families, then more or different mistuning patterns are needed to determine the change in modulus of elasticity. The concept is demonstrated in Fig. 7. The plot shows that using only mistuning families one through four yields the line with circles. These results demonstrate that family six is not accurately represented and that more or different families must be used. The line with diamonds shows that an improved identification of variations in the modulus of elasticity are obtained by using mistuning families one, two, five, and six. Note that all mistuning families had low residuals in this case, including families two and four.

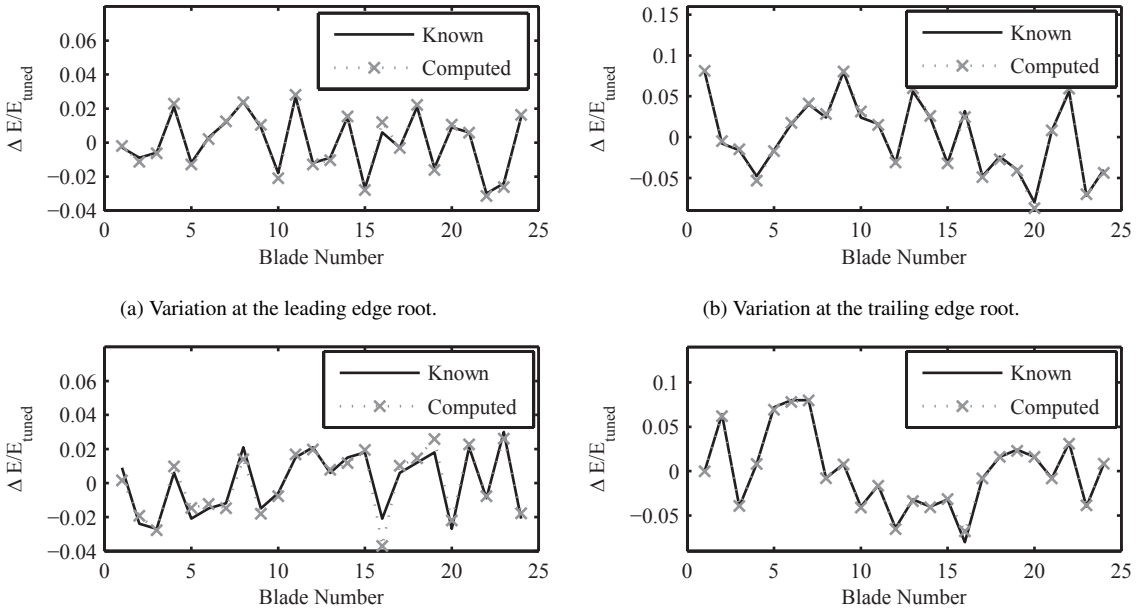

(a) Variation at the leading edge root.

(b) Variation at the trailing edge root.

(c) Variation at the leading edge tip.

(d) Variation at the trailing edge tip.

Figure 6. Identification of modulus of elasticity variations at specified blade locations using MistID results.

B. Iterative Measurement Point Selection for Mistuning Identification

The algorithm for the proposed iterative method is shown in Fig. 8. This approach features two improvements compared to the previous work of the authors.[23] First, for the forward problem, the forced response analysis is used

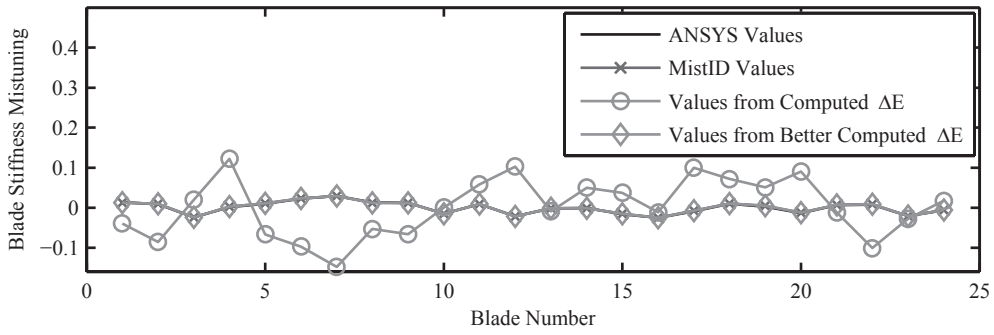

Figure 7. Improvement of modulus of elasticity variation using residual calculations for 6th CB mode.

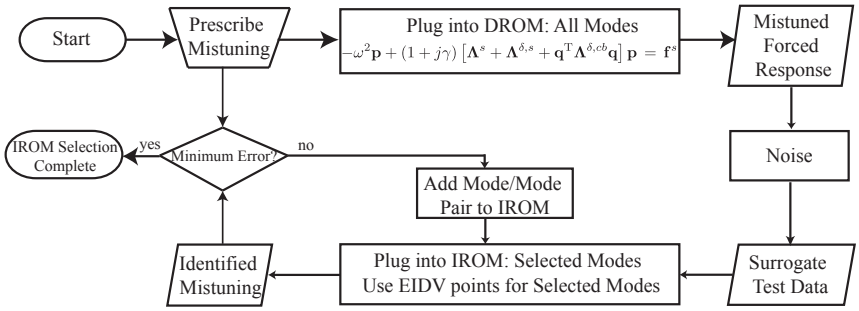

Figure 8. Flow diagram for IROM evaluation using surrogate data and EIDV measurement iteration.

to generate surrogate data for the identification procedure. This takes into account the error that comes from the transformation from physical to modal coordinates. The second improvement compared to the previous work is the iteration on the EIDV measurement points which is an essential part of identifying mistuning in higher frequency ranges.

Considering again Fig. 5, the necessity of being selective for the limited amount of measurement points becomes obvious. Although these are not the system modes that EIDV uses to determine the measurement points, it is important to remember that CMM uses the cantilevered blade mode to approximate the blade portion of the system modes. In Fig. 9a, the mistuning results are presented for family six using a valid but suboptimal EIDV measurement point (per blade) for the given frequency range, and then the optimal point for the IROM selected modes. It is clear that results with lower accuracy are obtained if a suboptimal point is used. Figure 9b shows the mistuning error over all possible IROM sizes. The DROM forced response surrogate data used with the mistuning algorithm determines that the optimal set of modes happens to be all of the modes in the regions. It should be noted that it is coincidental that all of the modes are used.

The ANSYS generated forced response results for suboptimal EIDV measurement points indicate that a different mode set would be used and the minimum error would be only slightly less than the error for the optimal point (at that number of modes). However, it is clear that, with the optimal EIDV measurement point in conjunction with the optimal number of modes, the error is minimized with the given set of measurement points. It should also be noted that the DROM surrogate data is obtained using several random mistuning patterns to compute the forced response. Then, the algorithm selects the worse error out of those patterns for a given number of IROM modes. This explains why the DROM curve has more error than the optimal curve.

IV. Conclusions

Mistuning ID and reduced-order model updating in higher frequency ranges has been discussed. The identification of multiple mistuning patterns and how these affect modeling results at higher modes was considered. The specific geometric location of blade imperfections that cause mistuning becomes more important at higher frequencies, because

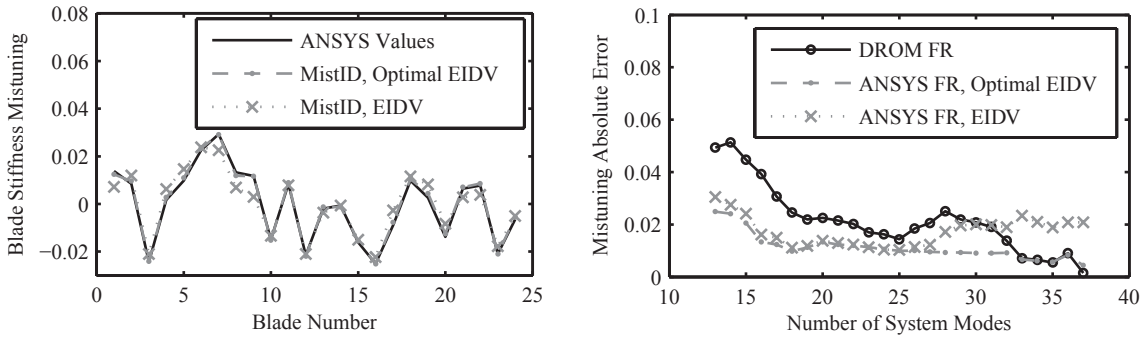

(a) Model updating parameters for 6th CB mode

(b) Mistuning error vs. mode number for 6th CB mode

Figure 9. Justification of iterative EIDV procedure using 6th cantilevered blade mode.

the wavelength decreases and the blade response features higher amplitudes in smaller regions of each blade. Thus, it becomes necessary to determine how each mode is affected by mistuning by identifying a (unique) set of mistuning values for each blade mode type. Using the CMM-based mistuning identification method, it is possible to identify multiple mistuning patterns. It is also possible to subsequently determine the locations of the physical mistuning sources. A method has also been proposed to improve the accuracy of such results using surrogate mistuning patterns and computing residuals using the identified physical parameters. The importance of the multiple mistuning patterns on the blisk modeling at higher modes has been highlighted.

Due to more complicated blade response shapes at higher frequencies, the limitation of experimentally measuring only a few points per blade is very important. To select points that well represent the system mode shapes used in the CMM model, the EIDV procedure is used in an iterative manner for multiple sets of candidate modes in order to determine the best EIDV measurement points. This is done by first using a set of EIDV measurement points chosen from a candidate mode set. The mistuning identification procedure computes the EIDV measurement points for each considered IROM mode set. This allows for a better set of measurement points for the modes actually used in the identification procedure. These measurement points are more sensitive to mistuning and better able to represent the mode shapes used in the reduced-order model for predictions.

Overall, the approaches presented in this work significantly enhance the identification and modeling of mistuning in higher frequency ranges. Therefore, this work helps enable the design and analysis of blisks throughout the entire operating range.

Acknowledgments

This work was supported by GE Aviation through the University Strategic Alliance (USA) program, with Sergio Filippi and Steve Manwaring as the technical contacts and George Sandusky as the program manager. In this paper there is no data representative of an actual GE blisk. We would like to especially thank Sergio Filippi for his fruitful conversations and suggestions regarding this research.

References

[1]Castanier, M. P., Óttarsson, G., and Pierre, C., "A Reduced Order Modeling Technique for Mistuned Bladed Disks," *Journal of Vibration and Acoustics*, Vol. 119, No. 3, 1997, pp. 439–447.

[2]Bladh, R., Castanier, M. P., and Pierre, C., "Component-Mode-Based Reduced Order Modeling Techniques for Mistuned Bladed Disks—Part I:Theoretical Models," *Journal of Engineering for Gas Turbines and Power*, Vol. 123, No. 1, 2001, pp. 89–99.

[3]Bladh, R., Castanier, M. P., and Pierre, C., "Component-Mode-Based Reduced Order Modeling Techniques for Mistuned Bladed Disks—Part II: Application," *Journal of Engineering for Gas Turbines and Power*, Vol. 123, No. 1, 2001, pp. 100–108.

[4]Yang, M.-T. and Griffin, J. H., "A Reduced-Order Model of Mistuning Using A Subset of Nominal System Modes," *Journal of Engineering for Gas Turbines and Power*, Vol. 123, No. 4, 2001, pp. 893–900.

[5]Feiner, D. M. and Griffin, J. H., "A Fundamental Model of Mistuning for a Single Family of Modes," *Journal of Turbomachinery*, Vol. 124, No. 4, 2002, pp. 597–605.

[6]Lim, S., Bladh, R., Castanier, M. P., and Pierre, C., "A Compact, Generalized Component Mode Mistuning Representation for Modeling Bladed Disk Vibration," *Collection of Technical Papers — AIAA/ASME/ASCE/AHS/ASC Structures, Structural Dynamics and Materials Conference*, Vol. 2, AIAA, Reston, VA, 2003, pp. 1359–1380.

[7]Lim, S., Bladh, R., Castanier, M. P., and Pierre, C., "Compact, Generalized Component Mode Mistuning Representation for Modeling Bladed Disk Vibration," *AIAA Journal*, Vol. 45, No. 9, 2007, pp. 2285–2298.

[8]Mignolet, M. P. and Lin, C.-C., "Identification of Structural Parameters in Mistuned Bladed Disks," *Journal of Vibration and Acoustics*, Vol. 119, No. 3, 1997, pp. 428–438.

[9]Pichot, F., Thouverez, F., Jezequel, L., and Seinturier, E., "Mistuning Parameters Identification of a Bladed Disk," *Key Engineering Materials*, Vol. 204-205, 2001, pp. 123–132.

[10]Judge, J., Pierre, C., and Ceccio, S. L., "Experimental Identification of Mistuning in Blisks," *Proceedings of the 6th National Turbine Engine High Cycle Fatigue Conference*, Universal Technology Corporation, Dayton, OH, 2001.

[11]Judge, J., Pierre, C., and Ceccio, S. L., "Experimental Validation of Mistuning Identification Techniques and Vibration Predictions in Bladed Disks," *Proceedings of the International Forum on Aeroelasticity and Structural Dynamics*, Madrid, Spain, 2001.

[12]Judge, J. A., Pierre, C., and Ceccio, S. L., "Mistuning Identification in Bladed Disks," *Proceedings of the International Conference on Structural Dynamics Modelling*, Madeira, Portugal, 2002.

[13]Pierre, C., Judge, J., Ceccio, S. L., and Castanier, M. P., "Experimental Investigation of the Effects of Random and Intentional Mistuning on the Vibration of Bladed Disks," *Proceedings of the 7th National Turbine Engine High Cycle Fatigue Conference*, Universal Technology Corporation, Dayton, OH, 2002.

[14]Judge, J. A., *Experimental Investigations of the Effects of Mistuning on Bladed Disk Dynamics*, Ph.D. thesis, The University of Michigan, Ann Arbor, 2002.

[15]Feiner, D. M. and Griffin, J., "A Completely Experimental Method of Mistuning Identification in Integrally Bladed Rotors," *Proceedings of the 8th National Turbine Engine High Cycle Fatigue Conference*, Universal Technology Corporation, Dayton, OH, 2003, pp. 1.1–1.13.

[16]Kim, N. E. and Griffin, J., "System Identification in Higher Modal Density Regions of Bladed Disks," *Proceedings of the 8th National Turbine Engine High Cycle Fatigue Conference*, Universal Technology Corporation, Dayton, OH, 2003, pp. 1.68–1.82.

[17]Feiner, D. and Griffin, J., "Mistuning Identification of Bladed Disks Using a Fundamental Mistuning Model—Part I: Theory," *Journal of Turbomachinery*, Vol. 126, No. 1, 2004, pp. 150–158.

[18]Feiner, D. and Griffin, J., "Mistuning Identification of Bladed Disks Using a Fundamental Mistuning Model—Part II: Application," *Journal of Turbomachinery*, Vol. 126, No. 1, 2004, pp. 159–165.

[19]Lim, S., Castanier, M. P., and Pierre, C., "Mistuning Identification and Reduced-Order Model Updating for Bladed Disks Based on a Component Mode Mistuning Technique," *Proceedings of the 9th National Turbine Engine High Cycle Fatigue Conference*, Universal Technology Corporation, Dayton, OH, 2004.

[20]Lim, S.-H., *Dynamic Analysis and Design Strategies for Mistuned Bladed Disks*, Ph.D. thesis, The University of Michigan, Ann Arbor, April 2005.

[21]Li, J., Pierre, C., and Ceccio, S. L., "Validation of a New Technique for Mistuning Identification and Model Updating Based on Experimental Results for an Advanced Bladed Disk Prototype," *Evaluation, Control and Prevention of High Cycle Fatigue in Gas Turbine Engines for Land, Sea and Air Vehicles (Meeting Proceedings RTO-MP-AVT-121)*, NATO Research and Technology Organisation, Neuilly-sur-Seine, France, 2005, pp. 36–1–36–16.

[22]Song, S. H., Castanier, M. P., and Pierre, C., "System Identification of Multistage Turbine Engine Rotors," *Proceedings of the ASME Turbo Expo*, Vol. 5, American Society of Mechanical Engineers, New York, 2007, pp. 569–582.

[23]Madden, A., Castanier, M., and Epureanu, B., "Reduced-Order Model Construction Procedure for Robust Mistuning Identification of Blisks," *AIAA*, Vol. 46, No. 11, 2009, pp. 2890–2898.

[24]Kammer, D. C., "Sensor Placement for On-Orbit Modal Identifiction and Correlation of Large Space Structures," *Journal of Guidance, Control, and Dynamics*, Vol. 14, No. 2, 1991, pp. 251–259.

[25]Penny, J. E. T., Friswell, M. I., and Garvey, S. D., "Automatic Choice of Measurement Locations for Dynamic Testing," *AIAA Journal*, Vol. 32, No. 2, 1994, pp. 407–414.

[26]Yang, M.-T. and Griffin, J. H., "A Normalized Modal Eigenvalue Approach for Resolving Modal Interaction," *Journal of Engineering for Gas Turbines and Power*, Vol. 119, No. 3, 1997, pp. 647–650.